Sphere Packing Analysis for Performance Trade-off in Joint Communications and Sensing-Part II: Fourier Analysis of Volume

Husheng Li, Zhu Han, H. Vincent Poor

ICC 2024 - IEEE International Conference on Communications | 978-1-7281-9054-9/24/$31.00 ©2024 IEEE | DOI: 10.1109/ICC51166.2024.10623040

***Abstract*—The technology of joint communications and sensing (JCS) is expected to prevail in 6G wireless networks. There exists a performance trade-off between the functions of communications and sensing in JCS. One effective approach to analyze the trade-off in JCS is to consider the level sets of a given performance metric of sensing as the signaling space of communication codewords. Then, performance bounds can be obtained for communications using the approach of sphere packing. The principle for generic sensing performance metric has been studied in the first part of this paper. In the second part of this paper, the concrete cases of sensing performance metrics, namely the signal-to-noise ratio (SNR) and integrated sidelobe level (ISL), are studied. The problems are turned into the volume evaluation for the intersection of a (elliptic) sphere (the quadratic approximation of the level set) and a hyperplane (the constraint on the total transmit power). They are solved by using the theory of Fourier-transform-based volume evaluation of convex sets. It is found that the optimal waveform is not unique, thus providing free lunch (although not plenty of) for communications. Another finding is that the communication data rate increases logarithmically with respect to the sensing performance metric degradation.**

I. Introduction

In joint communications and sensing (JCS), both functions are carried by the same waveform: the forward propagation of the electromagnetic (EM) wave sends communication messages to the destination; upon significant reflectors, the EM wave brings back the environment information for sensing in the backward propagation. JCS is expected to substantially improve the spectrum and power efficiency, thus being a promising technology in 6G wireless communication networks.

Due to the different goals and different preferences, there exist conflicts between communications and sensing in JCS. It is of critical importance to identify and assess the conflicts and the corresponding performance trade-offs between the two functions. An effective approach for evaluating the performance trade-off in JCS is to identify the set of waveforms that achieve a certain performance requirement for sensing (e.g., given a tolerance on the sensing performance degradation due to data communications). Then, the communication data rate is determined by the number of codewords (namely the selected transmit waveforms) in the set. The sphere-packing approach is effective [1] for bounding the number of codewords by evaluating the volume of the signal space.

H. Li is with the School of Aeronautics and Astronautics, and the School of Electrical and Computer Engineering (email: husheng@purdue.edu). Z. Han is with the Department of Electrical Engineering, University of Houston (email: zhan2@uh.edu). H. V. Poor is with the Department of Electrical Engineering, Princeton University (email: poor@princeton.edu). This work was supported by the National Science Foundation under grants 2052780, 2135286, 2109295 and 2128455.

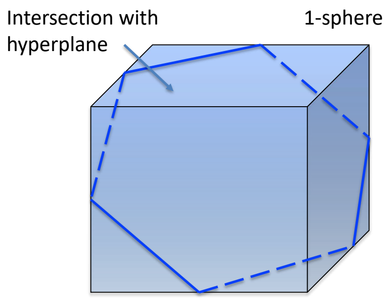

Fig. 1: Intersection of convex set.

In the first paper of this paper [2], we have proposed a generic principle for quantifying the communication-sensing trade-off in JCS. The problem boils down to the volume evaluation of the intersection of a (elliptic) sphere (the quadratic approximation of the level set) and a hyperplane (the constraint on the total transmit power). The first study of this kind was credited to Laplace, who calculated the volume of a unit cube in $\mathbb{R}^n$ intersected by a central hyperplane perpendicular to the vector $\left(\frac{1}{\sqrt{n}}, ..., \frac{1}{\sqrt{n}}\right)$, as illustrated in Fig. 1. Besides many peculiar phenomena of this volume evaluation in the high dimensional space, it is found that such a kind of problems is deeply related to Fourier analysis [3]. In this second part of this paper, we use the above machinery to study the communication-sensing trade-off, when the sensing performance is evaluated using signal-to-noise ratio (SNR) and integrated sidelobe level (ISL). It is found that the optimal waveform is not unique, thus providing free lunch (although insufficient) for communications. Another finding is that the communication data rate increases logarithmically with respect to the sensing performance metric degradation.

The remainder of this paper is organized as follows. The system model is introduced in Section II. Then, the analysis on the sensing performance metrics of SNR and ISL is carried out in Sections III and IV, respectively. The numerical results and conclusions are provided in Sections V and VI, respectively.

II. System Model

The system model has been introduced in the first part of this paper [2]. Here we restate it for self-containedness. The continuous-time signal is denoted by $x(t)$, whose N samples (fast time chips) of $x(t)$ within one pulse are denoted by $\mathbf{x} = (x_1, ..., x_N)^T$. The transmit power, normalized by the pulse duration, is denoted by P_t, while the power allocated to each sub-carrier is denoted by $\{P_{t,n}\}_{n=1,...,N}$. The total available bandwidth is W. We consider a data matrix that consists of M successive pulses (the slow time dimension). The signal within the data matrix is denoted by the time domain signal vectors $\bar{\mathbf{x}} = (\mathbf{x}_1, ..., \mathbf{x}_M)$, or equivalently the frequency domain vectors $\bar{\mathbf{X}} = (\mathbf{X}_1, ..., \mathbf{X}_M)$. We assume that the reflection of the radar target is frequency-selective. The frequency response is denoted by $H(j\omega)$, whose discrete-time samples are given by $H_k = H(j2\pi(f_c+(k-1)W/N))$, $k = 1, ..., N$.

III. Geometric Trade-off Analysis: SNR

In this section, we consider the SNR as the performance metric of sensing and analyze the sphere-packing-based performance bounds for communications.

A. Optimal Waveforms

We notice that only the power spectral density (PSD) is specified for the optimal waveform and the phase spectrum is free for selection. Therefore, for maximizing SNR, it is more convenient to carry out coding independently at different frequencies (as subcarriers in OFDM). According to Eq. (5) in the first part of this paper [2], we require

$$P_{t,n}^{opt} = E\left[|X_{mn}|^2\right] \propto |H_n|^2. \quad (1)$$

Therefore, the signal can be considered as in a complex sphere $\mathcal{S}^{MN}_{\sqrt{MP_t}} \subset \mathbb{C}^{MN}$ with dimension MN and radius $\sqrt{MP_t}$[1] (since the sum pulse-duration-normalized power of the M symbols is MP_t). Hence, the set of optimal waveforms for sensing is given by (where $\mathcal{P}_n$ is the projection to the signal over the n-th subcarrier)

$$\begin{aligned}\mathbf{\Sigma}_x &= \left\{\mathbf{z}|\mathbf{z} \in \mathcal{S}^{MN}_{\sqrt{MP_t^{opt}}}, \mathcal{P}_n(\mathbf{z}) = \mathcal{S}^{M}_{\sqrt{MP_{t,n}^{opt}}}, n = 1, ..., N\right\} \\ &= \prod_{n=1}^{N} \mathcal{S}^{M}_{\sqrt{MP_{t,n}^{opt}}},\end{aligned} \quad (2)$$

[1]Here, we allow transmitting without peak rate. Due to the concentration phenomenon, most of the volume will be concentrated close to the surface, when MN is sufficiently large.

which is essentially the product of N M-dimensional complex balls in $\mathbb{C}^M$ with radius $\left\{\sqrt{MP_{t,n}^{opt}}\right\}_{n=1,...,N}$.

The volume of complex sphere $\mathcal{S}^{M}_{\sqrt{MP_{t,n}^{opt}}}$ is equal to that of real sphere $\mathbb{S}^{2M}_{\sqrt{MP_{t,n}^{opt}}}$. Therefore, the volume of the feasible waveform set $\mathbf{\Sigma}_x$, whose real-valued dimension is $2MN$, is given by the standard formula of sphere volume:

$$V(\mathbf{\Sigma}_x) = \frac{\pi^{MN}}{\Gamma^N(M+1)} M^{MN} \prod_{n=1}^{N} (P_{t,n}^{opt})^M. \quad (3)$$

B. Suboptimal Waveforms

Now, we allow some slight deviation from the optimal power allocation $\{P_{t,n}^{opt}\}_{n=1,...,N}$ that maximizes the sensing SNR.

1) Constraint: We denote by $P_{t,n}$ the transmit power allocated to subcarrier n, and define the power deviation $\delta P_{t,n} = P_{t,n}^{opt} - P_{t,n}$ the deviation from the optimal power allocation, which is assumed to be small. Note that power deviation $\delta P_{t,n}$ should satisfy the following constraint on the deviation of transmit power:

$$\sum_{n=1}^{N} \delta P_{t,n} = 0, \quad (4)$$

due to the invariance of total transmit power.

2) Volume Analysis: Since the SNR is given by

$$\gamma = \frac{1}{N_0 W} \sum_{n=1}^{N} |H_n|^2 P_{t,n}, \quad (5)$$

where N_0 is the noise PSD, and the optimal SNR is given by

$$\gamma^{opt} = \frac{1}{N_0 W} \frac{\sum_{n=1}^{N} |H_n|^4 P_t}{\sum_{n=1}^{N} |H_n|^2}, \quad (6)$$

the level set corresponding to the SNR degradation is then given by

$$\sum_{n=1}^{N} |H_n|^2 \delta P_{t,n} \leq N_0 W \delta\gamma, \quad (7)$$

where $\delta\gamma$ is the maximal tolerable SNR degradation.

Therefore, the set of feasible $\{\delta P_{t,n}\}_{n=1,...,N}$ that result in tolerable SNR degradation is given by

$$\mathbf{\Sigma}_P = \mathcal{P}_{N-1} \cap \mathcal{C}_N, \quad (8)$$

where the subscript $N-1$ or N indicates the corresponding dimension, $\mathcal{P}_{N-1} = \mathbf{1}_N^{\perp}$ ($\mathbf{1}_N = (1, 1, 1, ..., 1)$) is a hyperplane[2], and $\mathcal{C}_N$ is a convex polytope defined as

$$\mathcal{C}_N = \left\{\sum_{n=1}^{N} |H_n|^2 \delta P_{t,n} \leq N_0 W \delta\gamma, P_{t,n}^{*} - \delta P_{t,n} \geq 0\right\}. \quad (9)$$

[2]$\mathbf{x}^{\perp}$ means the hyperplane perpendicular to the vector $\mathbf{x}$.

The volume evaluation of the intersection of the hyperplane $\mathcal{P}_{N-1}$ and the convex polytope $\mathcal{C}_N$ is difficult, due to the lack of symmetry and the complexity of the face structure. Therefore, we consider deriving a lower bound by noticing

$$\left|\sum_{n=1}^{N}|H_n|^2\delta P_{t,n}\right| \leq \sum_{n=1}^{N}|H_n|^2|\delta P_{t,n}|. \tag{10}$$

Therefore, when $\delta\gamma$ is sufficiently small, we have

$$\mathcal{E}_N^{\|\cdot\|_1} = \left\{\delta P_{t,n}\left|\sum_{n=1}^{N}|H_n|^2||\delta P_{t,n}| \leq N_0 W\delta\gamma\right.\right\} \subset \mathcal{C}_N, \tag{11}$$

where $\mathcal{E}_N^{\|\cdot\|_1}$ is 1-norm ellipsoid. Therefore, we evaluate the volume of $\mathcal{P}_{N-1}$ and $\mathcal{E}_N^{\|\cdot\|_1}$ to obtain a lower bound for the volume of feasible power allocation.

To facilitate the analysis, we rescale the coordinates, define $x_n = |H_p|^2\delta P_{t,n}$ and evaluate $\text{Vol}(\tilde{\mathcal{P}}_{N-1}) \cap \tilde{\mathcal{E}}_N^{\|\cdot\|_1}$, where the rescaled sets are given by

$$\begin{cases} \tilde{\mathcal{P}}_{N-1} = \left(\frac{1}{|H_1|^2}, \frac{1}{|H_2|^2}, \ldots, \frac{1}{|H_N|^2}\right)^{\perp} \\ \tilde{\mathcal{E}}_N^{\|\cdot\|_1} = \left\{x_n \left| \sum_{n=1}^{N}|x_n| \leq N_0 W\delta\gamma\right.\right\} \end{cases}. \tag{12}$$

Since $\tilde{\mathcal{E}}_N^{\|\cdot\|_1}$ is now a 1-norm sphere, we apply Theorem 1 in the first part of this paper [2], and obtain

$$\begin{aligned} & Vol(\tilde{\mathcal{P}}_{N-1}) \cap \tilde{\mathcal{E}}_N^{\|\cdot\|_1} \\ = \ & \frac{(N_0 W\delta\gamma)^N}{\pi(N-1)\Gamma(N-1)}\int_0^{\infty}\prod_{k=1}^{N}\gamma_1\left(\frac{t}{|H_k|^2}\right)dt, \end{aligned} \tag{13}$$

where the term $(N_0 W\delta\gamma)^N$ is due to the radius $N_0 W\delta\gamma$ and the dimension N.

Notice that the Fourier transform $\gamma_1(\omega) = \mathcal{F}\left(e^{-|t|}\right) = \frac{2}{\omega^2+1}$. Therefore, the challenge is how to evaluate the integral of the product of N terms. For simplicity, we assume that all the values of $|H_k|^2$ are distinct. Thanks to the trick of partial fraction expansion [4], we have

$$\begin{aligned} & \int_0^{\infty}\prod_{k=1}^{N}\frac{2|H_k|^2}{t^2+|H_k|^2}dt \\ = \ & \int_0^{\infty}\sum_{k=1}^{N}\frac{A_k}{t^2+|H_k|^2}dt \\ = \ & \sum_{k=1}^{N}\int_0^{\infty}\frac{A_k}{t^2+|H_k|^2}dt \\ = \ & \sum_{k=1}^{N}\frac{A_k}{|H_k|^2}\left(\tan^{-1}\left(\frac{x}{|H_k|^2}\right)\Big|_{x=\infty} - \tan^{-1}\left(\frac{x}{|H_k|^2}\Big|_{x=0}\right)\right) \\ = \ & \sum_{k=1}^{N}\frac{A_k\pi}{2|H_k|^2}, \end{aligned} \tag{14}$$

where the residue A_k of each term is given by

$$A_k = \prod_{l=1}^{N}\frac{2|H_l|^2(x+|H_k|^2)}{x+|H_l|^2}\Bigg|_{x=-|H_k|^2} \tag{15}$$

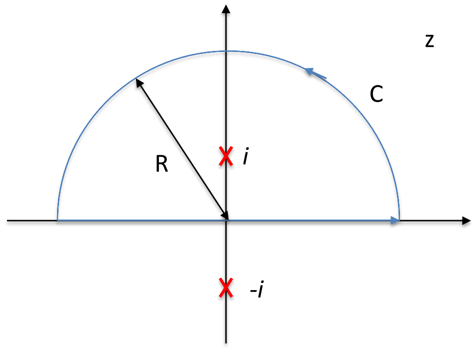

Fig. 2: Contour of integral.

Substituting (14) into (23), we obtain

$$\begin{aligned} & Vol(\tilde{\mathcal{P}}_{N-1}) \cap \tilde{\mathcal{E}}_N^{\|\cdot\|_1} \\ = \ & \frac{2(N_0 W\delta\gamma)^N}{(N-1)\Gamma(N-1)}\sum_{k=1}^{N}\frac{A_k}{|H_k|^2}, \end{aligned} \tag{16}$$

Note that the above derivation is based on the assumption that $|H_k|^2 \neq |H_l|^2$ for $k \neq l$; otherwise, the partial fraction expansion does not hold. Here we consider the other extreme case in which $|H_k|^2 = 1$ for all k, namely the frequency manitude response is flat. In this case, we need to evaluate the following integral:

$$\int_0^{\infty}\left(\frac{2}{t^2+1}\right)^N dt = \lim_{R\to\infty}\frac{1}{2}\oint_C\frac{2^N}{(z^2+1)^N}dz, \tag{17}$$

where the contour C is shown in Fig. 2. We notice that there are two N-order poles at i and $-i$, where i is surrounded by C. Note that the integral over the arc vanlishes as $R \to \infty$, since

$$\begin{aligned} \int_{C:|z|=R}\frac{1}{(z^2+1)^N}dz &\leq \int_{C:|z|=R}\frac{1}{|z^2+1|^N}dz \\ &\leq \int_{C:|z|=R}\frac{1}{(R^4-2R^2+1)^{\frac{N}{2}}} \\ &= \frac{\pi R}{(R^4-2R^2+1)^{\frac{N}{2}}} \to 0, \end{aligned} \tag{18}$$

as $R \to \infty$. Note that the second inequality is due to

$$\begin{aligned} \left|(a+jb)^2+1\right|^2 &= |a^2-b^2+1+2jab|^2 \\ &= (a^2-b^2+1)^2+(2ab)^2 \\ &= (a^2+b^2)^2+1+2a^2-2b^2 \\ &\geq (a^2+b^2)^2+1-2b^2 \\ &\geq R^4-2R^2+1. \end{aligned} \tag{19}$$

Then, according to the Residue Theorem in complex analysis [5], we have

$$\frac{1}{2}\oint_C\frac{2^N}{(z^2+1)^N}dz = j\pi 2^N Res(f,i), \tag{20}$$

where $f = \frac{1}{(z^2+1)^N}$ and the residue at the N-th order pole i is given by

$$\begin{aligned} Res(f,i) &= \frac{1}{(N-1)!}\frac{d^{N-1}}{dz^{N-1}}\frac{1}{(z+j)^N}\bigg|_{z=j} \\ &= \frac{(2N-1)!}{((N-1)!)^2}\frac{(-1)^{N-1}}{(z+j)^{2N-1}}\bigg|_{z=j} \\ &= \frac{(2N-1)!}{((N-1)!)^2}\frac{(-1)^{N-1}}{(2j)^{2N-1}} \\ &= \frac{(2N-1)!}{((N-1)!)^2}\frac{(-1)^{N-1}}{j2^{2N-1}j^{2N-2}} \\ &= \frac{(2N-1)!}{((N-1)!)^2}\frac{1}{j2^{2N-1}}, \end{aligned} \tag{21}$$

which leads to

$$\begin{aligned} \frac{1}{2}\oint_C \frac{2^N}{(z^2+1)^N}dz &= j\pi 2^N \times \frac{(2N-1)!}{((N-1)!)^2}\frac{1}{j2^{2N-1}} \\ &= \frac{2\pi(2N-1)!}{((N-1)!)^2 2^N}. \end{aligned} \tag{22}$$

Substituting (22) into (23), we obtain

$$\begin{aligned} & Vol(\tilde{\mathcal{P}}_{N-1}) \cap \tilde{\mathcal{E}}_N^{\|\cdot\|_1} \\ = & \frac{2(N_0 W\delta\gamma)^N(2N-1)!}{(N-1)2^N\Gamma(N-1)((N-1)!)^2}, \end{aligned} \tag{23}$$

Since the set $\tilde{\mathcal{P}}_{N-1}$ has been scaled, we need to rescaled it back to the original coordinate. Hence, in summary, we obtain the following lower bounds for the space of power allocation:

$$\begin{aligned} & \text{Vol}(\mathbf{\Sigma}_P) \geq \\ & \frac{2(N_0 W\delta\gamma)^N}{(N-1)\Gamma(N-1)\prod_{n=1}^N |H_n|^2}\sum_{k=1}^N \frac{A_k}{|H_k|^2}, \end{aligned} \tag{24}$$

for the case of unequal channel gains, and

$$\begin{aligned} & \text{Vol}(\mathbf{\Sigma}_P) \geq \\ & \frac{2(N_0 W\delta\gamma)^N(2N-1)!}{(N-1)(2\pi)^N\Gamma(N-1)((N-1)!)^2\prod_{n=1}^N |H_n|^2}, \end{aligned} \tag{25}$$

for the case of equal channel gains.

C. Sphere Packing Analysis

1) Optimal SNR: As we have discussed, the waveform corresponding to the optimal SNR is not unique, thus providing a free lunch for data communications. According to Eq. (10) in the first paper of this paper, the maximum communication data rate in JCS, given the minimum distance $d_{\min}$, is lower bounded by

$$\begin{aligned} R_{fix} &\geq \log_2\left[\frac{V(\Sigma)}{V(B_{d_{\min}})}\right] \\ &= \log_2\left[\frac{\Gamma(MN+1)M^{MN}}{\Gamma^N(M+1)}\prod_{n=1}^N\left(\frac{P_{t,n}^{opt}}{d_{\min}^2}\right)^M\right] \end{aligned} \tag{26}$$

2) Suboptimal SNR - Lower Bound: The volume analysis results in (24) and (25) provide lower bounds. According to (11) in the first part of this paper [2], we have

$$\begin{aligned} R_{flx} &\geq \log_2 \frac{V(\Sigma_P)}{V\left(B_{\frac{d_{\min}^2}{M}}\right)}\frac{V(\Sigma)}{V(B_{d_{\min}})} \\ &= R_{fix} + \log_2 C_0 + N\log_2 \delta\gamma, \end{aligned} \tag{27}$$

where the offset C_0 equals

$$C_0 = \frac{2(MN_0W)^N(2N-1)!\Gamma\left(\frac{N}{2}-1\right)}{(N-1)(2\pi)^N\Gamma(N-1)((N-1)!)^2\prod_{n=1}^N |H_n|^2 d_{\min}^2}. \tag{28}$$

We observe that the degradation of SNR provides an extra data rate in a logarithmic manner. Note that the above results are valid when $\delta\gamma$ is sufficiently small, such that the power allocations in the spheres are nonnegative, while $d_{\min}$ is even smaller such that the power allocation space contains one or more spheres. Therefore, the above conclusion applies for slight sensing performance degradation and high SNR.

3) Suboptimal SNR - Upper Bound: Note that we may still derive upper bounds for the volume evaluation of $\mathbf{\Sigma}_P$, such that we can derive upper bounds for the codebook size similarly to the Hamming bound. Notice that the inequality (7) is equivalent to

$$\delta P_{t,n} \leq \frac{1}{|H_n|^2}\left(N_0 W\delta\gamma - \sum_{l=1,l\neq n}^N |H_l|^2\delta P_{t,l}\right), \tag{29}$$

for $n = 1, ..., N$, which implies

$$\begin{aligned} |\delta P_{t,n}| &\leq \frac{1}{|H_n|^2}\left(N_0 W\delta\gamma + \sum_{l=1,l\neq n}^N |H_l|^2|\delta P_{t,l}|\right) \\ &\leq \frac{1}{|H_n|^2}\left(N_0 W\delta\gamma + \sum_{l=1,l\neq n}^N |H_l|^2|P_{t,l}^{opt}|\right), \end{aligned} \tag{30}$$

for $n = 1, ..., N$, which is equivalent to

$$\max_n |\delta P_{t,n} \leq \Theta, \tag{31}$$

where $\Theta = \max_n \frac{1}{|H_n|^2}\left(N_0 W\delta\gamma + \sum_{l=1,l\neq n}^N |H_l|^2|P_{t,l}^{opt}|\right)$. Therefore, the following set

$$\mathcal{C}_N \subset \mathcal{E}_N^{\|\cdot\|_\infty} = \left\{\delta P_{t,n}\middle| \max_n |\delta P_{t,n} \leq \frac{\Theta}{|H_n|^2}\right\}, \tag{32}$$

which is a ball of norm $\|\cdot\|_\infty$ and provides an upper bound for the volume of $\mathbf{\Sigma}_P$. Due to the limited space of the paper, we omit the corresponding volume analysis, which is also an application of Theorem 1 in the first part of this paper [2], [3].

IV. Geometric Trade-off Analysis: ISL

In this section, we focus on the sensing performance based on ISL, which employs similar mathematical tool for volume evaluation and sphere packing to the previous section. The definition of ISL can be found in the first part of this paper.

A. Optimal Waveforms

We first consider the optimal waveforms in both the time and frequency domains.

1) Time Domain: We first assume that ISL is the performance metric for radar sensing and denote by $\mathbf{x}^{opt}$ the optimal sequence of signal that achieves the minimum ISL (namely the optimal performance). Obviously, $e^{j\theta}\mathbf{x}$ obtained from adding a phase change θ does not change the ISL, since the phase change is canceled out when calculating the ISL. Therefore, there exists a free lunch for the coding of communications. However, it is difficult for further analysis in the time domain.

2) Frequency Domain: It is easier to study the optimal waveform in the frequency domain of the discrete-time signals. It is well known that the autocorrelation function in Eq. (2) in the first part of this paper and the PSD $|X(j\Omega)|^2$ are a pair of Discrete-Time Fourier Transform (DTFT), based on the Wiener-Khintchine Theorem [6]. According to the Parseval's Theorem [6], we have

$$\sum_{m=-(N-1)}^{N-1} |r[m]|^2 = \frac{1}{2\pi}\int_{-\pi}^{\pi} |X(j\Omega)|^4 d\Omega. \tag{33}$$

Meanwhile, according to the Parseval's Theorem for the DTFT pair (x, X), we have

$$r[0] = \sum_{n=-(N-1)}^{N-1} |x[n]|^2 = \frac{1}{2\pi}\int_{-\pi}^{\pi} |X(j\Omega)|^2 d\Omega. \tag{34}$$

We notice that the normalized ISL ξ is given by

$$\begin{aligned}
\xi &= \frac{1}{r^2[0]}\left(\sum_{m=-(N-1)}^{N-1} |r[m]|^2 - r^2[0]\right) \\
&= \frac{1}{r^2[0]} \times \frac{1}{2\pi}\int_{-\pi}^{\pi} |X(j\Omega)|^4 d\Omega \\
&- \frac{1}{r^2[0]}\left(\frac{1}{2\pi}\int_{-\pi}^{\pi} |X(j\Omega)|^2 d\Omega\right)^2 \\
&= \frac{1}{{}^2 r[0]}\left(E\left[|X(j\Omega)|^4\right] - E^2\left[|X(j\Omega)|^2\right]\right) \\
&= \frac{Var\left[|X(j\Omega)|^2\right]}{E^2[|X(j\Omega)|^2]},
\end{aligned} \tag{35}$$

which turns out to be the standard deviation of the PSD of the signal $\{x[n]\}_{n=1,...,N}$.

Take N samples on the spectrum $X(j\Omega)$, which are denoted by $X[1], ..., X[n]$. We observe that the change of phase in $X[n]$ does not change the ISL. Therefore, the space of optimal waveforms is essentially $[-\pi, \pi]^N$. The volume assessment is the same as that of the SNR analysis, which is omitted here due to the limited space.

B. Suboptimal Waveforms

Now, we relax the optimality on the waveforms and consider possible degradation of sensing performance. We denote by $P_{t,n} = |X[n]|^2$ the power of the n-th sample in the PSD $|X(j\Omega)|^2$. According to (35), the ISL is approximated given by

$$\xi \approx \frac{Var[\{P_{t,n}\}_{n=1,...,N}]}{E^2[\{P_{t,n}\}_{n=1,...,N}]} = \frac{N^2 Var[\{P_{t,n}\}_{n=1,...,N}]}{P_t^2}, \tag{36}$$

where the optimal PSD is the uniform distribution $P_{t,n}^* = \frac{p_t}{N}$.

Following the methodology of analyzing the communication-sensing trade-off in SNR, we first calculate the first- and second-order derivatives of ISL:

$$\begin{cases} \frac{\partial}{\partial P_{t,n}} ISL = \frac{2NP_{t,n}}{P_t^2} - \frac{2}{P_t} \\ \frac{\partial^2}{\partial P_n^2} ISL = \frac{2N}{P_t^2} \\ \frac{\partial^2}{\partial P_{t,n}\partial P_m} ISL = 0, \text{ if } m \neq n. \end{cases} . \tag{37}$$

Due to the optimality of the performance at the PSD $\{P_{t,n}^{opt}\}_{n=1,...,N}$, we consider the second order approximation:

$$\frac{2N}{P_t^2}\sum_{n=1}^{N} \delta P_{t,n}^2 \leq \delta\xi, \tag{38}$$

where $\delta\xi$ is the tolerable performance degradation of ISL.

Therefore, when the tolerable performance decay is $\delta\xi$, the feasible power deviations $\{\delta P_{t,n}\}$ are within the following N-dimensional elliptic sphere:

$$\mathcal{E}_N = \left\{\{\delta P_{t,n}\}\middle| \sum_{n=1}^{N} \delta P_{t,n}^2 \leq \Delta_\xi\right\}, \tag{39}$$

where $\Delta_\xi = \frac{\delta\xi P_t^2}{2N}$. Meanwhile, we also have the constraint of total transmit power, namely $\{\delta P_{t,n}\}$ should lie on the $N-1$ dimensional hyperplane

$$\mathcal{P}_{N-1} = \left\{\{\delta P_{t,n}\}\middle| \sum_{n=1}^{N} \delta P_{t,n} = 0\right\}. \tag{40}$$

Then, the set of feasible power deviations is the unit $N-1$-dimensional intersection of the $N-1$-hyperplane $\mathcal{P}_{N-1}$ and the N-dimensional sphere $\mathcal{E}_N$, namely

$$\mathcal{F}_{N-1}^{ISL} = \mathcal{P}_{N-1} \cap \mathcal{E}_N, \tag{41}$$

as illustrated in Fig. 3.

Fortunately, intersection is an $N-1$-dimensional sphere, whose volume is given by

$$Vol(\mathcal{F}_{N-1}) = \frac{(2\pi)^{\frac{N-1}{2}}}{\Gamma\left(\frac{N-1}{2}\right)}(\Delta_\xi)^{\frac{N-1}{2}}. \tag{42}$$

The sphere-packing analysis is similar to that of the SNR case. The detailed analysis is omitted due to the limited space. The rule-of-thumb is that the data rate increases with an extra term $\frac{N-1}{2}\log_2 \Delta_\xi$.

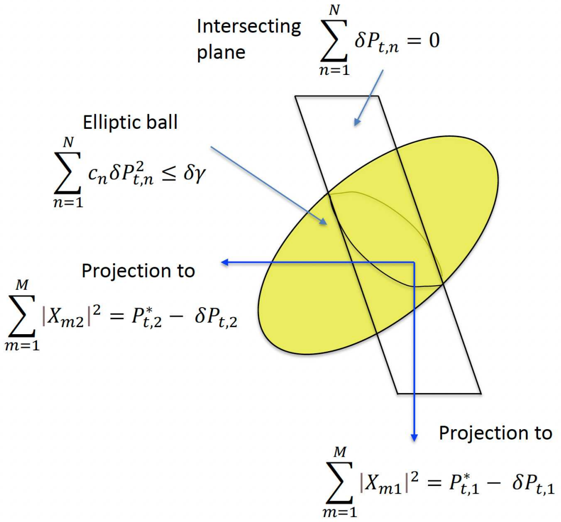

Fig. 3: Illustration of intersection and projection.

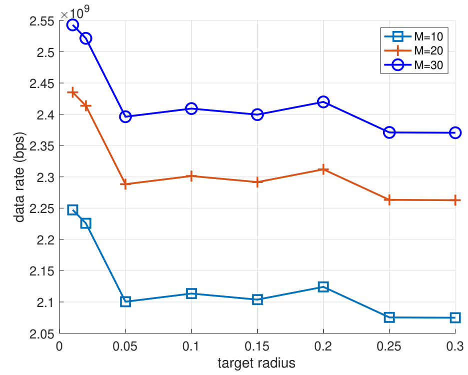

Fig. 4: Data rate with waveform maximizing SNR.

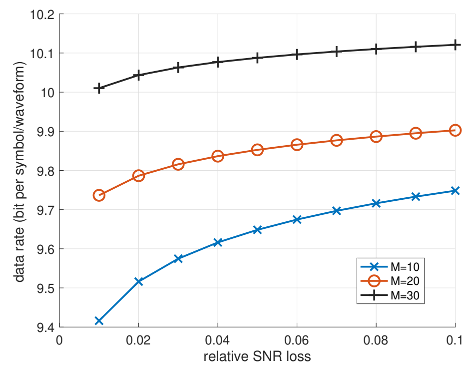

Fig. 5: Data rate versus relative SNR drop.

V. Numerical Results

As the first part of this paper, we consider a JCS system in the 2.5GHz band with a bandwidth of 400MHz. We assume that a ball of radius 0.3m, as a the target, is located 100m away from the JCS transceiver. The noise PSD is assumed to be 10^{-17}, and the signal path loss in the round trip is 20dB.

Due to the limited space, we consider only the sensing performance metric of SNR. In Fig. 4, we plotted the bound of data rate in (26), obtained from the sphere packing argument, versus different values of M and target radius. We observe that, even fixing the optimal waveform, the data rate can still be very high (in the order of Gbps), in the ideal case. We also notice that the data rate is increased by 10% or so, as M is increased from 10 to 30, which demonstrates the benefit of joint coding across different slow data blocks. An interesting observation is that, as the target radius increases, the data rate drops by approximately 10% and then keeps slow decreasing. The reason for the dependency on target radius is that small targets incur less frequency selectivity, thus resulting in flatter signal PSD and greater communication channel capacity.

In Fig. 5, we plot the lower bound in (27) for the data rate as a function of relative sensing SNR reduction. We observe that the data rate increases slowly as the sensing performance deteriorates. For example, when $M = 30$, the data rate increases for about 1% as the sensing SNR drops for 10%. Therefore, for the system setting in this paper, it is more desirable to stay close to the optimal power allocation and encode the communication data in the phase.

VI. Conclusions

In this paper, we have studied the fundamental trade-off between communications and sensing in JCS systems. Based on the generic principle introduced in the first part of this paper, we have started from the set of optimal sensing waveforms, in terms of SNR or ISL, and discussed the volume of optimal waveforms for constructing the communication codebook. Then, we have relaxed the optimality and studied the volume of level sets of sensing, given the specified sensing performance degradation. Bounds for communication data rate have been derived based on the volume analysis and sphere packing argument. Numerical simulation results have shown that the sensing performance degradation is compensated by linearly increasing communication data rate, which justifies the theoretical validity of JCS.

References

[1] J. H. van Lint, *Introduction to Coding Theory*. Springer, 1992, vol. GTM 86.
[2] H. Li, Z. Han, and H. V. Poor, "Sphere packing analysis for performance trade-off in joint communications and sensing-part i: General principle," in *submitted to IEEE Global Communications Conference (Globalcom)*, 2023.
[3] A. Koldobsky, *Fourier Analysis in Convex Geometry*. American Mathematical Society, 2005.
[4] M. J. Roberts, *Signals and Systems: Analysis Using Transform Methods & MATLAB*. McGraw Hill, 2017.
[5] E. M. Stein and R. Shakarchi, *Complex Analysis*. Princeton University Press, 2003.
[6] W. Fuller, *Introduction to Statistical Time Series*. Wiley, 1996.